Physica E 43 (2011) 702–706

Contents lists available at ScienceDirect

Physica E

journal homepage: www.elsevier.com/locate/physe

On detecting absolute quantum mechanical phase differences with superfluid interferometers

Yuki Sato [a,*], Richard Packard [b]

[a] The Rowland Institute at Harvard, Harvard University, Cambridge, MA 02142, USA
[b] Physics Department, University of California at Berkeley, Berkeley, CA 94720, USA

ARTICLE INFO

Available online 1 August 2010

ABSTRACT

We show through numerical simulations that absolute quantum mechanical phase differences could be observed using an asymmetric superfluid quantum interference grating. By balancing the dynamic range and the degree of change required per period in an interference pattern, a device could be optimized and used to probe heretofore inaccessible quantum subtleties. We make connections to experimental results and discuss possible applications for such systems.

1. Introduction

Superfluid matter-wave interferometers [1,2] have revealed some fascinating physical phenomena that are accompanied by quantum mechanical phase shifts. For example, phase shifts due to absolute rotation (the Sagnac effect [3,4]) revealed the connection of matter waves to a nonrotating inertial frame, and the phase gradient associated with superfluid flow [5] demonstrably linked the macroscopic wavefunction concept with the two-fluid description of the Bose–Einstein condensate [6]. In addition, there are predicted phase shifts arising from novel interactions such as an Aharonov–Bohm phase shift in neutral matter [7], which could suggest a more general interpretation of Berry's phase phenomena.

Superfluid interferometers provide us with a novel method to probe aspects of fundamental physics by registering changes in phase difference in response to an external influence. However, a measurement of "absolute" phase differences has always remained elusive. A double-path superfluid interferometer (with two weak links configured as in a conventional superconducting quantum interference device (dc-SQUID [8,9])) cannot determine the initial phase difference offset that may be present when the device is first viewed. Such "phase biases" may be due to external fields or trapped vortices and persistent current within the superfluid. This initial offset, $\Delta\phi_0$, cannot be determined for it is physically indistinguishable from $\Delta\phi_0 \pm 2\pi n$ with an interference pattern that is 2π periodic in $\Delta\phi$. Having a means to measure absolute phase differences (i.e. without the modulo $2\pi n$) between two locations would be important in understanding the nature of quantum phase and the quantum mechanics that governs it. Here we show that this situation can be remedied and absolute phase differences could be directly observed with an asymmetric superfluid quantum interference grating. We report the results of our numerical simulation and make a connection to the first superfluid interference grating reported in Ref. [10].

2. Double-path superfluid interferometry

The superfluid state of ^{4}He is described by a macroscopic order parameter of the form $\psi = |\psi|e^{i\phi}$, where ϕ is a quantum mechanical phase [6]. A superfluid quantum interference device consists of two "weak links" placed in a loop of superfluid ^{4}He analogous to a dc-SQUID. A weak link in this case is an array of nanoscale apertures whose dimension is matched to the temperature-dependent healing length (coherence length) of superfluid ^{4}He near the superfluid transition temperature T_λ. A typical weak link is a 100×100 array of nominally ~ 70 nm apertures, constructed by e-beam lithography in a ~ 60 nm thick silicon nitride membrane. These dimensions are selected to match the superfluid healing length at $T_\lambda - T \approx 5$ mK. An array of apertures remains phase coherent and is used to increase the total mass flow to a detectable level. One example of experimental apparatus used as an interferometer is schematically represented in Fig. 1. See Refs. [1,2,5] for other configurations with various complexities. Nanofabrication processes for aperture arrays are described in detail in Ref. [11].

Consider a tube filled with superfluid helium with a uniform phase gradient (eg. due to flowing superfluid) along its axis (depicted in Fig. 2a). To observe the phase drop due to this gradient and investigate the nature of external phase shifting influence, one can make use of a superfluid quantum interference

* Corresponding author.
E-mail address: sato@rowland.harvard.edu (Y. Sato).

1386-9477/$ - see front matter © 2010 Elsevier B.V. All rights reserved.
doi:10.1016/j.physe.2010.07.033

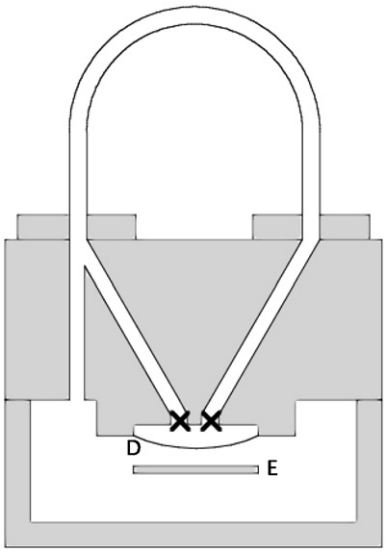

Fig. 1. Typical experimental apparatus. Crosses indicate positions of weak links. The inside is filled with superfluid ^{4}He and the entire apparatus is immersed in a temperature-regulated bath of liquid helium. A flexible diaphragm (D) and fixed electrode (E) are used to apply DC pressure difference (and hence DC chemical potential difference) across the weak links. The diaphragm also forms the input element of a sensitive microphone based on superconducting electronics that are not shown.

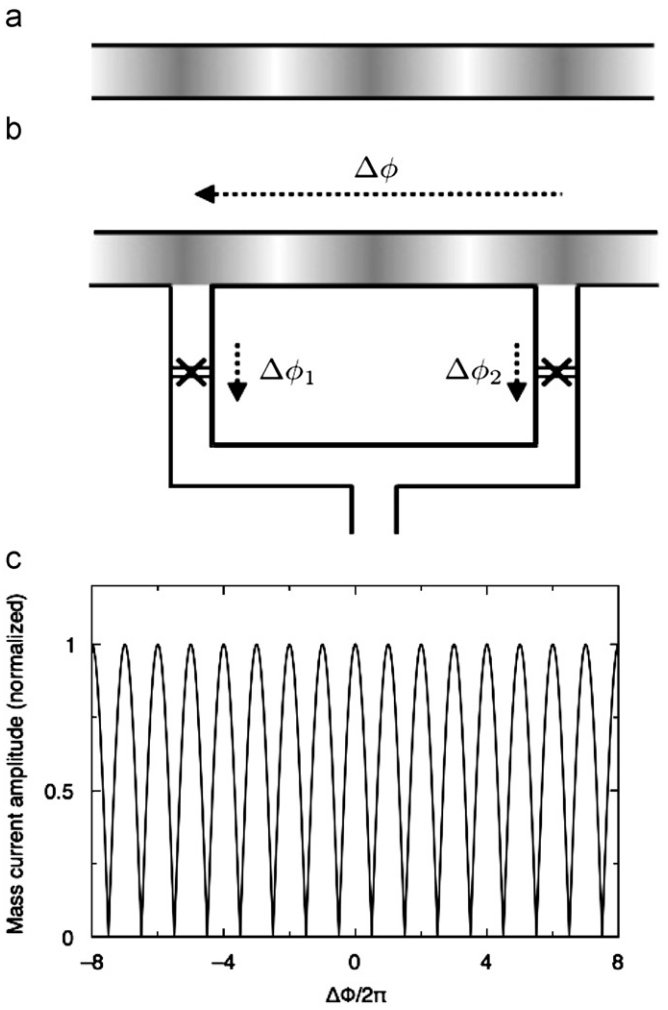

Fig. 2. (a) A tube filled with superfluid helium. A uniform phase gradient (due to some external influence such as flow) exists along the axis. (b) The tube in (a) is configured as part of a double-path interferometer to measure $\Delta\phi$. (c) Simulated interference pattern for identical weak link arrays.

device. Fig. 2b shows how the tube in Fig. 2a can be included as part of a double-path interferometer loop to monitor the phase difference $\Delta\phi$. Crosses indicate superfluid weak links, and $\Delta\phi_1$ and $\Delta\phi_2$ represent phase drops across the junctions. These phase differences $\Delta\phi_1$ and $\Delta\phi_2$ evolve in response to a chemical potential difference $\Delta\mu$ applied across the junctions [6]. For constant $\Delta\mu$, phase difference across a weak link evolves as $\Delta\phi_1 = (\Delta\mu/\hbar)t$.

Well below T_λ, superfluid within the aperture arrays is characterized by a linear current-phase relation with discrete 2π phase slips. Closer to T_λ, it follows a sinelike dc-Josephson current phase relation [12]. In both regimes, when a constant DC chemical potential difference $\Delta\mu$ is applied across the aperture arrays, fluid within each array exhibits AC mass current oscillation [13–15] at a Josephson frequency $\Delta\mu/h$. In experiments, we place a highly sensitive displacement sensor [16] (not shown in Fig. 1) in the vicinity of weak links to monitor the combined Josephson mass current oscillation from multiple junctions.

For a double-path configuration depicted in Fig. 2b, the total mass current oscillation (from two weak link arrays) is

$$I_0 \sin\Delta\phi_1 + I_0 \sin\Delta\phi_2, \tag{1}$$

assuming that the two junctions have the same oscillation amplitude I_0. We now impose a phase integral condition along a closed loop of superfluid: $\Delta\phi + \Delta\phi_1 - \Delta\phi_2 = 0$. Using this relation, the total oscillation amplitude as a function of $\Delta\phi$ can be written as [2]

$$2I_0\left|\cos\frac{\Delta\phi}{2}\right|. \tag{2}$$

For simulation purposes, we simply rewrite Eq. (1) as $I_0\sin(2\pi f_J t) + I_0\sin(2\pi f_J t + \Delta\phi)$. The expected amplitude of this oscillation as a function of $\Delta\phi$ is plotted in Fig. 2c. The pattern has been numerically generated by adding two sine waves with the same frequency with a phase lag $\Delta\phi$, taking a power spectrum of the combined signal, and plotting the square root of the power under the Josephson peak (in frequency space) as a function of $\Delta\phi$. The amplitude has been normalized. The modulation has the form described by Eq. (2). Note the simple cyclic nature of the interference pattern. Although this periodicity is very useful in giving the interferometer a wide dynamic range, as described earlier it gives no information about absolute phase differences. The double-path quantum interference patterns observed in superfluid experiments can be seen in Refs. [1,2,5]. In practice, two weak links are not exactly identical due to the limitations of nanofabrication technology. This results in different oscillation amplitudes for two arrays, eliminating complete destructive interference.

3. Symmetric grating superfluid interferometry

Since superfluid interferometry relies on measuring the change in mass current oscillation amplitude as a function of $\Delta\phi$, the sensitivity of the device is proportional to the slope of the interference pattern at its steepest point. The sensitivity can be increased by placing more than two arrays in parallel thus narrowing the peaks in the interference pattern. In the field of superconducting devices, Feynman suggested [17] the importance

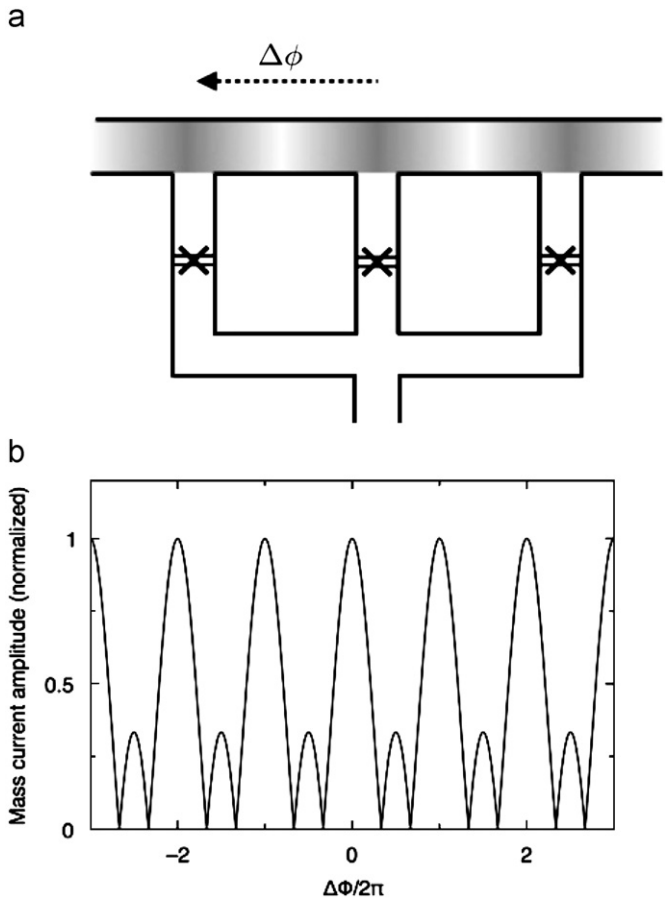

Fig. 3. (a) Symmetric three-slit grating structure and (b) simulated interference pattern.

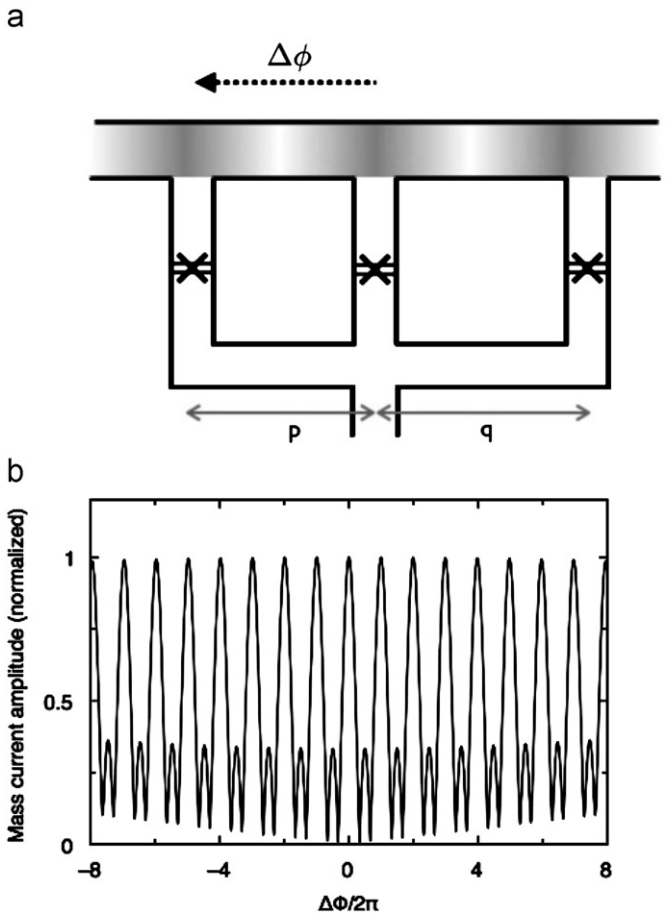

Fig. 4. (a) Asymmetric three-slit grating structure and (b) simulated interference pattern.

of such a device as a magnetometer (referred to as a superconducting quantum interference grating (SQUIG)), and it was first demonstrated experimentally with six point contacts in 1966 [18]. A similar configuration can be employed for a superfluid interferometer. Fig. 3a shows three weak links spaced equally in a multi-slit interference grating configuration. The expected interference pattern for this particular structure (simulated as described above for three sine waves) is shown in Fig. 3b. The similarity to a three-slit optical interference pattern [19] can be seen. The sensitivity of the device is increased due to the narrowing of the peaks. If N identical weak links (each with current amplitude I_0) are used in the grating, the total oscillation amplitude should modulate as [20,21]

$$I_0\left|\frac{\sin(N\Delta\phi/2)}{\sin(\Delta\phi/2)}\right|. \tag{3}$$

Note that the above relation reduces to Eq. (2) when $N=2$. Numerical analysis of Eq. (3) shows [21] that the slope at the steepest part of the interference pattern $|dI/d\Delta\phi|_{\max}$ from a grating structure increases as $\propto N^2$ where $N>2$.

We note that the interference pattern shown in Fig. 3b still has a period of 2π. Therefore, as in the double-path case, this symmetric grating configuration only allows differential measurements on quantum mechanical phase differences. A key to being able to make absolute measurements hinges on somehow making the period of interference pattern much longer than 2π. The first multi-slit interference pattern observed in superfluid helium (from four weak links) is reported in Ref. [10].

4. Asymmetric grating superfluid interferometry

One can control the periodicity of overall interference pattern by introducing asymmetry into the system. Fig. 4a shows three weak links in a grating structure (as in the case with the previous section) but this time unequally spaced. Here p and q are defined to be the distances between neighboring phase probing locations. The simulated interference pattern is shown in Fig. 4b. For this example, we have chosen $q/p=1.013$. Notice that the pattern slowly evolves as $\Delta\phi$ is increased. Unequal spacing in the grating introduces asymmetry and breaks the simple 2π cyclic nature of the interference pattern. It is now possible to tell the cycles apart, making the detection of absolute phase differences feasible.

We have parameterized the evolution of interference pattern by the ratio of adjacent peak heights β (ie. the height of the second peak divided by that of the first peak, fourth divided by the third, and so on) and plotted it as a function of $\Delta\phi$ for four different values of q/p in Fig. 5. The solid line for $q/p=1$ is what one would expect for a symmetric grating configuration (as in Fig. 3). Constant β means that one cannot tell the difference from cycle to cycle in the interference pattern making it impossible to detect absolute phase differences. In contrast, as one makes $q/p\neq 1$, the parameter β starts to change as a function of $\Delta\phi$.

We point out that the interference pattern simulated in Fig. 4b eventually repeats itself. This behavior is apparent in Fig. 5, which clearly shows periodic modulation of β in $\Delta\phi$. The period depends on the value q/p, and it is $\sim 800\pi$ for $q/p=1.005$, and $\sim 400\pi$ and $\sim 280\pi$ for $q/p=1.01$ and 1.015, respectively. Periodicity of β in $\Delta\phi$ determines the largest phase difference one can measure with

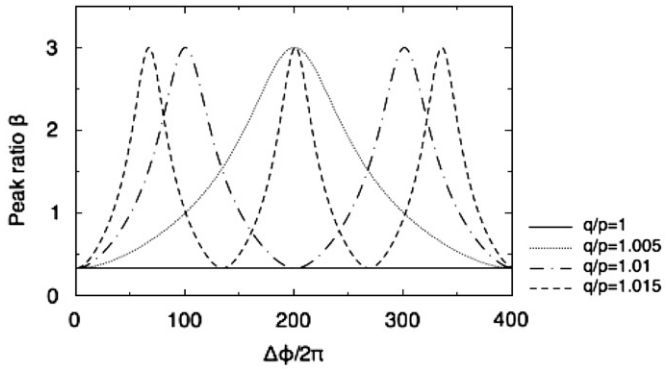

Fig. 5. Parameterization of evolving interference pattern for an asymmetric three-junction system. Peak ratio β as a function of $\Delta\phi$ is shown for four different values of q/p. The flat horizontal line is for the case $q/p=1$.

an asymmetric system as an absolute gauge. For example, if one uses an asymmetric grating with $q/p=1.013$ with an interference pattern shown in Fig. 4b, one can obtain the absolute phase difference by measuring the peak height ratio β as long as the expected phase difference of interest is below $\sim 300\pi$. We point out that these ranges can be made much longer by changing the grating geometry and also by adding more weak links. In principle, we want the interference pattern to never repeat itself so that the measurement on absolute phase differences can be done with a very wide dynamic range. However, we do not want the pattern to evolve too slowly. We need the interference pattern to change its shape sufficiently over a phase difference of 2π so that it would be possible to distinguish $\Delta\phi_0$ from $\Delta\phi_0 \pm 2\pi$. Using more weak links in a grating and spacing them all unequally can increase the period of modulation dramatically and very quickly (to a point where it almost never repeats itself). However, that also increases the complexity of the interference pattern, making it nontrivial to parameterize the pattern in a simple manner (as we have done above) and use that to tell the current position in the interference curve. Therefore, one needs to adjust the degree of geometrical asymmetry and number of weak links to make sure that the pattern evolves just enough (given the device's signal to noise ratio) while satisfying the dynamic range required for particular experiments. Maintaining a simple interference pattern also allows room for the application of flux-locking technique using superfluid heat current [22].

With a superfluid ^{4}He interferometer which operates mKs below T_λ, phase difference on the order of $\sim 500\pi$ in a tube whose length is $\sim 2\,\mathrm{cm}$ and cross sectional area of $\sim 0.04\,\mathrm{cm}^2$ corresponds to superfluid velocity of $\sim 1\,\mathrm{mm/s}$, very close to the extrinsic critical velocity [23]. Phase difference any larger than that would drive quantum turbulence rendering the interferometer useless. Therefore, the dynamic range of $\sim 300\pi$ (as in the example discussed above) might be sufficient for practical purposes. For the pattern shown in Fig. 4, the peak ratio parameter β changes most slowly near $\Delta\phi = 0$, and the change is $\sim 0.3\%$ comparing the ranges $0 \le \Delta\phi \le 2\pi$ and $2\pi \le \Delta\phi \le 4\pi$. In recent experiments, the smallest detectable current is on the order of 0.1 pg/s (in 1 s measuring time) with a typical signal size of 10 pg/s, which gives a S/N of about 100 in 1 Hz bandwidth. That should allow one to distinguish the interference pattern of $0 \le \Delta\phi \le 2\pi$ from that of $2\pi \le \Delta\phi \le 4\pi$ by sweeping a few cycles of the modulation curve while spending $\sim 10\,\mathrm{s/point}$ for the example shown in Fig. 4.

We point out that the effect of asymmetry simulated here is seen in the superfluid quantum interference grating (with four weak links) reported in Ref. [10]. The observed interference pattern increases its complexity as $\Delta\phi$ is increased. In designing that experiment, care was taken to minimize any geometrical differences. However, the finite width of four phase probing pipes introduced finite asymmetry, giving rise to the changing shape of the modulation pattern. The simulation results reported here show that instead of trying to minimize the asymmetry inherent in the system, one can purposefully introduce it and take advantage of it to optimize the device's sensitivity to absolute phase differences.

5. Possible applications

An asymmetric grating structure has been employed in superconducting systems in an attempt to make absolute measurements of magnetic field [24]. An equivalent device in superfluid system should allow the direct observation of absolute quantum mechanical phase differences, which would provide insights to equilibrium state and nonequilibrium dynamics of phase coherent quantum matter.

One interesting application of this asymmetric superfluid quantum interference grating might be the investigation of the initial phase offset that appears when the device is brought from normal to superfluid state through the transition temperature. When a device such as the one depicted in Fig. 3a goes through the transition, fluid in segments above and below the junctions become superfluid while the fluid within the junctions (nanoscale apertures) remains normal due to the suppressed transition temperature in a confined geometry. Then there are two quantum coherent regions (above and below the junctions) with unique quantum mechanical phases that are physically separated from each other. As the temperature is lowered further the two regions connect coherently. The phase difference that must have existed between the two separate regions should be registered in the interferometer signal. The statistical study of such phase differences could shed some light on the physical processes that govern the assignment of quantum phases to macroscopic coherent matter while giving insights to researchers investigating Kibble–Zurek scenarios [25,26] of formation of topological defects.

6. Conclusion

Using numerical simulations we have shown that absolute quantum mechanical phase differences could be observed with an asymmetric superfluid quantum interference grating. By balancing the dynamic range and the degree of change needed in interference patterns, the device could be optimized and used to probe some subtleties of the quantum world.

Acknowledgments

This work was supported in part by the National Science Foundation Grant DMR 0902147 and the Office of Naval Research.

References

[1] R.W. Simmonds, A. Marchenkov, E. Hoskinson, J.C. Davis, R.E. Packard, Nature 412 (2001) 55.
[2] E. Hoskinson, Y. Sato, R.E. Packard, Phys. Rev. B 74 (2006) 100509R.
[3] L.A. Page, Phys. Rev. Lett. 35 (1975) 543.
[4] S.A. Werner, J.L. Staudenmann, R. Colella, Phys. Rev. Lett. 42 (1979) 1103.
[5] Y. Sato, A. Joshi, R.E. Packard, Phys. Rev. Lett. 98 (2007) 195302.
[6] D.R. Tilley, J. Tilley, Superfluidity and Superconductivity, Institute of Physics, Bristol, 1990.
[7] H. Wei, R. Han, X. Wei, Phys. Rev. Lett. 75 (1995) 2071.
[8] K.K. Likharev, Dynamics of Josephson Junctions and Circuits, Academic Press, New York, 1986.

[9] J. Clarke, A.I. Braginski, The SQUID Handbook: Fundamentals and Technology of SQUIDs and SQUID Systems, Wiley-VCH, Weinheim, 2004.
[10] Y. Sato, A. Joshi, R.E. Packard, Phys. Rev. Lett. 101 (2008) 085302.
[11] A. Joshi, Y. Sato, R.E. Packard, J. Phys.: Conf. Ser. 150 (2009) 012018.
[12] K. Sukhatme, Y. Mukharsky, T. Chui, D. Pearson, Nature 411 (2001) 280.
[13] E. Hoskinson, Y. Sato, I. Hahn, R.E. Packard, Nat. Phys. 2 (2006) 23.
[14] Y. Sato, E. Hoskinson, R.E. Packard, Phys. Rev. B 74 (2006) 144502.
[15] E. Hoskinson, R.E. Packard, T. Haard, Nature 433 (2005) 376.
[16] H.J. Paik, J. Appl. Phys. 47 (1976) 1168.
[17] R.P. Feynman, R.B. Leighton, M. Sands, The Feynman Lectures on Physics, Addison-Wesley, New York, 1965.
[18] J.E. Zimmerman, A. Silver, Phys. Rev. 141 (1966) 367.
[19] A. Hudson, R. Nelson, University Physics, second ed., Saunders College Publishing, 1990.
[20] A. Th, A.M.D. Waele, W.H. Kraan, R.D.B. Ouboter, Physica 40 (1968) 302.
[21] J.T. Jeng, K.H. Huang, C.H. Wu, K.L. Chen, J.C. Chen, H.C. Yang, IEEE Trans. Appl. Supercond. 17 (2007) 691.
[22] Y. Sato, A. Joshi, R.E. Packard, Appl. Phys. Lett. 91 (2007) 074107.
[23] Y. Sato, A. Joshi, R.E. Packard, Phys. Rev. B 76 (2007) 052505.
[24] J. Oppenlander, T. Trauble, C. Haussler, N. Schopohl, IEEE Trans. Appl. Supercond. 11 (2001) 1271.
[25] W.H. Zurek, Nature 317 (1985) 505.
[26] A. Maniv, E. Polturak, G. Koren, Phys. Rev. Lett. 91 (2003) 197001.